DOI: 10.1002/adma.200602698

Mismatch Strain Induced Formation of ZnO/ZnS Heterostructured Rings**

By *Xiang Wu*, *Peng Jiang*,* *Yong Ding*, *Wei Cai*, *Si-Shen Xie*, and *Zhong Lin Wang**

Wurtzite-structured materials, such as ZnO, ZnS, GaN, etc., possess a common characteristic that is the existence of polar surfaces originated from cation- or anion-terminated surfaces. The polar surfaces have two unique features: the polar-charge induced formation of novel nanostructures as driven by minimizing energy; and the self-catalysis of cation terminated surface during growth.[1–3] The first characteristic leads to the formation of nanorings,[4] nanosprings,[5] nanohelices[6] and nanobows.[7] The second characteristic results in the formation of one-side toothed growth of nanocombs.[8,9] To date, these nanostructures have been mainly observed for a mono-composition object such as ZnO.[10]

The structure of ZnO can be described as a number of alternating planes composed of tetrahedrally coordinated O^{2-} and Zn^{2+} ions, stacked alternatively along the *c*-axis. The oppositely charged ions produce positively charged (0001)-Zn and negatively charged $(000\bar{1})$-O polar surfaces, resulting in a normal dipole moment and spontaneous polarization along the *c*-axis. If the thickness of the nanobelt defined mainly by the large {0001} surfaces is below ~20 nm, the electrostatic interaction energy arising from the polar charges can be strong enough to overcome the increase of elastic bending energy, resulting in the curly shape of the nanobelts, which is the origin for the formation of the nanosprings, nanorings, nanohelices and nanobows. Take the formation of nanospring as an example, our previous study shows that the inner surface of the nanospring can be either Zn^{2+} or O^{2-} and the dominant driving force for forming the curly shape is the electrostatic interaction; the difference in surface stress for the Zn-terminated and O-terminated surfaces, if any, is so small that plays little role in forming the observed nanostructures.[7]

In this paper, we present a new ring structure that is composed of heterostructured ZnO/ZnS, with tooth decoration exclusively at the inner surface. The formation mechanism of the heterostructured nanoring is attributed to the strain induced bending that arises mainly from the lattice mismatch between ZnO and ZnS. This new structure provides a new process for forming hierarchical nanostructures that could have interesting application in optoelectronics.

The ZnO/ZnS heterostructured nanorings were synthesized by thermal evaporating mixed ZnS and graphite powder possibly with the presence of residual oxygen. Field emission scanning electron microscopy (SEM) was firstly used to examine the morphology of the as-synthesized nanostructures. Figure 1a demonstrates a representative SEM image of the product, which reveals that many one-side tooth-like nanobelts are formed. Some of the nanobelts curled into circle shape, with the outer surfaces of the nanorings smooth, while the inner surfaces having inward-pointing teeth (see Fig. 1b), the diameter of the formed circle-like rings can be several micrometers. The bent nanobelts have an average thickness of 50 nm, width of 100 nm and length from several to several hundreds of micrometers (see Fig. 1c). The straight tooth-like belt nanostructures are obviously thicker than those curved and can achieve a thickness of ~100 nm. The teeth grown on the nanobelts un-uniformly distribute on one side of the nanobelts and have an average height of 150 nm and size of 50 nm (see Fig. 1d and e). An interesting phenomenon is that the teeth are always at the inner surface of the ring.

The intrinsic structure of the nanobelt and nanorings has been studied by transmission electron microscopy (TEM). Figure 2a shows a low magnification TEM image of the nanostructure. Figure 2a and b are a pair of bright-field and dark-field TEM images recorded from the same segment of a nanobelt. Tooth-like structure on one side of the nanobelt is clearly observed. The nanobelt exhibits a double layered heterostructure, and the teeth may have a direct connection with the lower layer (see the areas indicated by arrowheads). Energy-dispersive X-ray spectra (EDS) acquired using a 2 nm electron probe from a few selected areas as marked in Figure 2d indicate that the nanobelt is ZnO/ZnS heterostructure with the ZnS at the inner surface of the ring; the teeth are ZnO. Selected area electron diffraction (SAED) pattern (Fig. 2c) shows the epitaxial relationship between ZnO and wurtzite

[*] Prof. P. Jiang, Prof. Z. L. Wang, X. Wu
National Center for Nanoscience and Technology
Beijing 100080 (P.R. China)
E-mail: zhong.wang@mse.gatech.edu; pjiang_hlx@yahoo.com
Prof. Z. L. Wang, Dr. Y. Ding
School of Materials Science and Engineering
Georgia Institute of Technology
Atlanta, GA 30332-0245 (USA)
X. Wu, Prof. W. Cai
School of Materials Science and Engineering
Harbin Institute of Technology
Harbin 150001 (P.R. China)
Prof. S.-S. Xie
Institute of Physics
Beijing 100080 (P.R. China)

[**] The work was supported by the Scientic Research Foundation for the Returned Overseas Chinese Scholars, State Education Ministry; The National Natural Science Foundation of China; Opening research foundation of National Center for Nanoscience and Technology (NCNST), China and "973" National Key Basic Research Project (2003CB716900).

ADVANCED MATERIALS

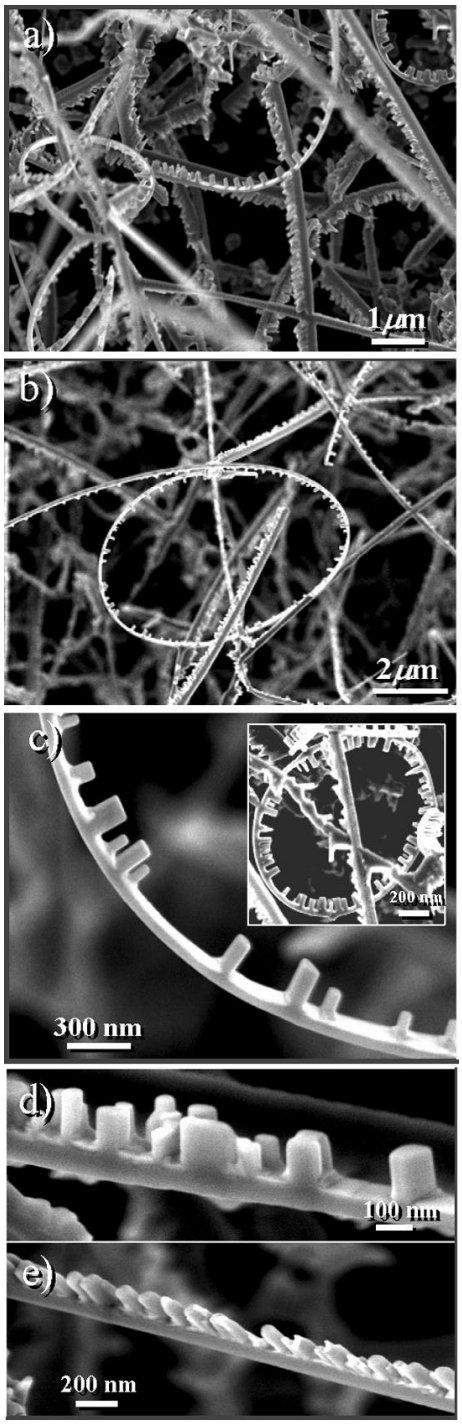

Figure 1. Typical morphologies of the as-synthesized tooth-like nanobelt structures. a) A low magnification SEM image showing a general morphology of the product. b) A curved morphology of the nanobelts. c) A high resolution SEM image of the curved nanobelts, some teeth can be clearly observed standing on the nanobelt; the insert demonstrates a circle of the nanobelt. d) and e) SEM images of straight tooth-like nanobelts.

ZnS: $[01\bar{1}0]ZnO \| [01\bar{1}0]ZnS$; $(0001)ZnS \| (0001)ZnS$. The nanobelt grows along $[01\bar{1}0]$ and the inner surface of the ring is (0001). The teeth are along [0001].

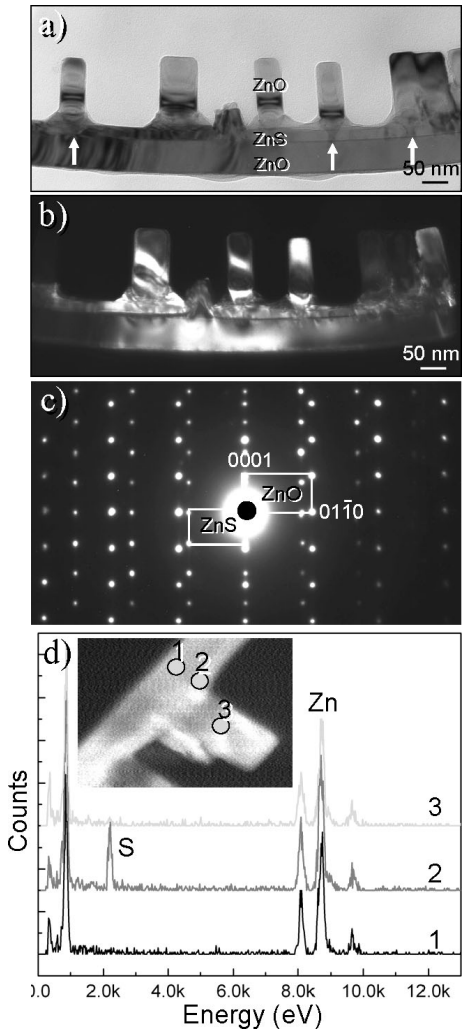

Figure 2. a) Low magnification bright field TEM image of a piece of a tooth-like nanobelt. The teeth grow exclusively at one side of the nanobelt. b) A dark field TEM image of the nanobelt. c) Corresponding selected area electron diffraction (SAED) pattern of the nanobelt, clearly indicating the epitaxial orientation relationship between ZnO and ZnS. d) Corresponding energy dispersive X-ray microanalysis (EDX) spectra acquired from the three labeled points (1, 2, 3), showing local compositions of ZnO, ZnS, and ZnO, respectively (see insert).

Zinc sulfide (ZnS) can be wurtzite or zinc blend depending on synthesis conditions. ZnS possesses two kinds of structural polymorphs: cubic sphalerite and hexagonal wurtzite. Bulk ZnS usually has the zinc blend crystal structure at room temperature. Once raising temperature beyond 1020 °C, bulk ZnS can transfer from the cubic zinc blend to a hexagonal wurtzite structure. The difference between the two structures is the sequence of atomic layer stacking parallel to the {111} (for cubic) or the {0001} (for hexagonal) planes in the forms of ABCABC··· or ABAB···.[11] The double crystal structures of ZnS material imply that more complicated nanostructures could occur for ZnS, such as the "Y" shape decorated hierarchical ZnS nanohelices.[12] The most amazing phenomenon is that the as-synthesized ZnS

nanobelts usually exhibit wurtzite structure although its thin films are zinc blend.[13]

To understand the origin of the curly shape of the ring, we have carried out a detailed study about the interfaces. A typical TEM image of single tooth-like heterostructure is displayed in Figure 3a, which clearly show that the tooth is rooted at the bottom ZnO layer, while the ZnS is formed at the side of the teeth. The corresponding electron diffraction pattern with streaking spots is due to the curly shape of the nanobelt. A dark-field image from another tooth shows consistent result (Fig. 3b). High magnification TEM image recorded from the interface between the ZnO and ZnS layer shows many mismatch dislocations separated evenly at an average interval of ~1.5 nm.

The lattice parameters for Wurtzite ZnO are $a = 0.32495$ nm and $c = 0.52069$ nm, and $a = 0.3811$ nm and $c = 0.6234$ nm for wurtzite ZnS. There exist a large lattice mismatch between ZnO and ZnS when forming an epitaxial layer. The lattice mismatch between $(01\bar{1}0)_{ZnO}$ and $(01\bar{1}0)_{ZnS}$ is 17.27 % (in reference to ZnO), which can give an array of mismatch edge dislocations at the interface at an interval of 1.91 nm, which agrees reasonably well to the experimentally observed separation of 1.5 nm. In such a case, the strain at the (0001) interface is mostly released by the creation of mismatch dislocations.

One possible reason for the bending may be due to thermal stress. Since ZnO has a smaller thermal expansion coefficient of $\alpha_{ZnO} = 2.9 \times 10^{-6}\,K^{-1}$ than that of ZnS ($\alpha_{ZnS} = 6.5 \times 10^{-6}\,K^{-1}$), an interface stress would be introduced when the sample was cooled from the growth temperature to room temperature. By a simple geometrical consideration, if the bending is soley introduced by thermal stress, the radius of the observed ring would be $R = t/2\Delta T(\alpha_{ZnS} - \alpha_{ZnO})$, where t is the thickness of the nanobelt, and $\Delta T = 600$ K is the drop in temperature at the growth site rather than the furnace temperature. For a general case, most of the nanobelts have an average thickness of t ~50 nm, the ring radius would be estimated to be R ~18 μm, which is much larger than the average radius of the ring of 1.5 μm. Therefore, thermal stress cannot be the dominant factor for forming the ring structure.

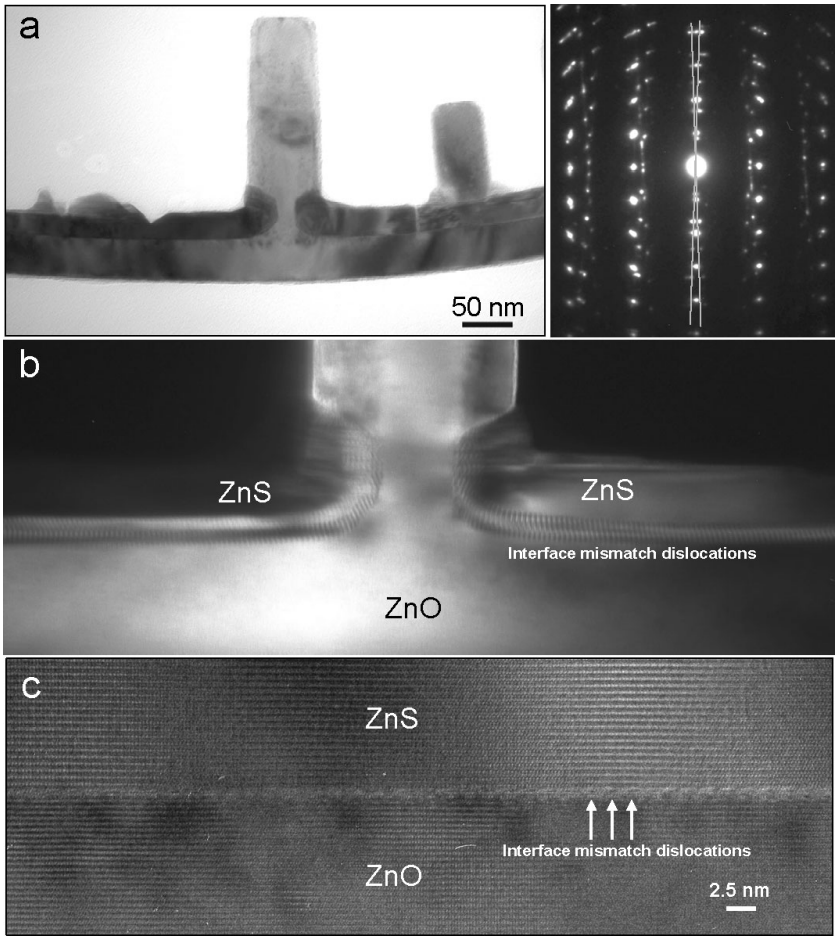

Figure 3. a) A bright field TEM image of one tooth on the nanobelt and corresponding SAED pattern, showing crystal lattice rotation induced by bending of the nanobelt. b) A magnified TEM image of root part of the tooth grown on the nanobelt. c) A high resolution TEM image of the nanobelt showing the (0001) interface between ZnO to ZnS. The interface dislocations are clearly resolved at the interface.

The lattice rotation can be directly proved by high resolution TEM images. Figure 4a shows a low magnification TEM image recorded at the end of a nanobelt with one tooth. Figure 4b is a high magnification TEM image of the local region. By tracking the *c*-axes directions for ZnO and ZnS, a clear rotation of the lattice for a ~7° is clearly identified between the tooth and the nanobelt. As we presented above, the strain at the (0001) interface is largely released. At the $(01\bar{1}0)$ interface, the lattice mismatch is 19.7 % (in reference to ZnO), and the mismatch is even bigger at the vicinity (see the selected area in Fig. 4b). Thus, the large local strain results in the relative rotation between the ZnO tooth and the ZnS layer. This is likely the reason that causes the bending of the nanobelt.

Based on our previous analysis of the comb-structure with teeth at one side of the nanobelt, the formation process of the ring can be described as follows (Fig. 5).[9] First, a ZnO nanobelt defined by {0001} and $\{2\bar{1}\bar{1}0\}$ surfaces is formed with a growth direction of $[01\bar{1}0]$ The (0001)-Zn terminated surface is chemically active and it self-catalyzes during growth, leading to the growth of the teeth. The $(000\bar{1})$-O terminated surface, however, is relatively chemically inert, thus, the surface may not initiate any growth along the side branches. Thus, the teeth tend to grow out of the (0001)-Zn terminated surface. Furthermore, we also found that the wurtzite ZnS has similar characteristic with the Zn terminated

ADVANCED MATERIALS

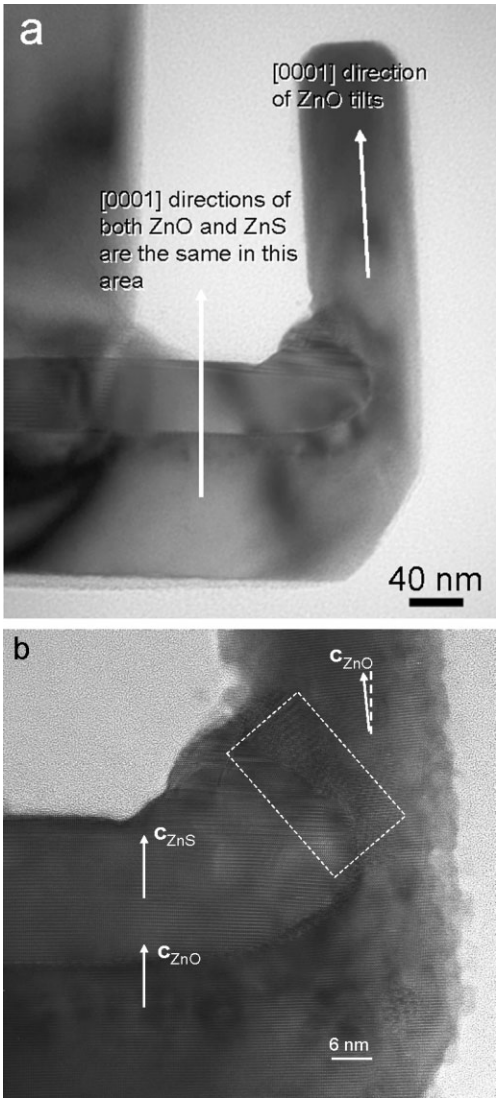

Figure 4. a) A bright field TEM image of the ZnO tooth formed on one end of the nanobelt. b) A high resolution TEM image of the bending region of the nanobelt. The arrowheads indicate the direction of the c-axis at the local regions.

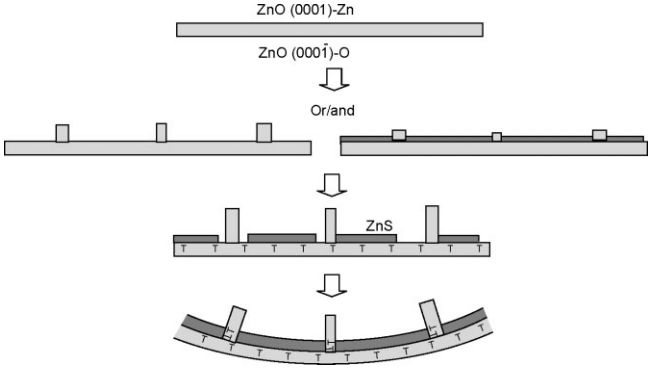

Figure 5. A schematic model illustration showing the formation process of a heterostructured ZnO/ZnS ring structure, where "T" indicates an interface mismatch edge-dislocation.

(0001) surface chemically active.[11] Thus, the ZnS film tends to grow on the (0001)-Zn surface of ZnO rather than the (000$\bar{1}$)-O terminated surface. In this case, a layer of ZnS film is probably formed on (0001)-Zn surface of the ZnO nanobelt because of the Zn-terminated surface has a higher catalytic activity and it tends to initiate the growth of ZnS. ZnO teeth are nucleated and grown after (or at about the same time) the formation of ZnS overlayer. ZnS film cannot form a large and uniform single crystal layer due to large lattice mismatch between ZnS and ZnO. A multi-nuclei growth as separated by the teeth is most likely. The presence of the teeth and the bending of the nanobelt help to release the lattice strain between ZnO and ZnS layers. Further, the teeth grow along [0001]. With considering the larger lattice parameters for ZnS than those of ZnO, the bending introduces a compressive strain for ZnS and a tensile strain for ZnO. This is why that the nanobelt tends to bend in a way that the inner surface is ZnS and the [0001] teeth are at the inner surface of the loop. Moreover, if the thickness of the nanobelt is large, the interface strain may not be sufficient to bend the nanobelt. In such a case, a straight ribbon with teeth at one side is formed.

In the literature, strain induced formation of rings have been reported for semiconductors thin films. By growing semiconductor multilayer thin films on a solid substrate, lifting the film can result in the formation of springs due to the mismatch strain[14,15] existing at the interface between the layers, such as Si/SiGe,[16] InGaAs/GaAs[17] and SiGe/Si/Cr.[18]

In summary, we have synthesized a novel heterostructured ZnO/ZnS ring. The formation process of the ring has been investigated, and is attributed due to the strain induced bending that arises mainly from the lattice mismatch between ZnO and ZnS. This growth model is in consistent to the electrostatic model proposed previously about the formation of nanorings, nanosprings and nanohelix, but it shows the dominant contribution from interface strain in the ring formation for such a special case. The ring structure of ZnO/ZnS provides an ideal candidate for investigate optoelectronics of ring structured II-VI semiconductors.

Experimental

The synthesis of the ZnO(teeth)/ZnS(nanobelt)/ZnO(nanobelt) sandwich nanobelts was performed in a vacuum tube furnace. A quartz tube was used for the synthesis. 1 g commercial ZnS plus graphite powder was held in an alumina boat and was positioned at the center of the tube furnace. A P-type Si wafers in a quartz boat were located in downstream region of the tube. The whole system was sealed and pumped to a pressure of 1 Torr. Then, the furnace was heated up to 900 °C at a 20 °C min^{-1} rate. High-purity Argon was aerated into the tube at a flow rate of 100 standard cubic centimeters per minute at a pressure of 300 Torr. The system was kept at 900 °C for 1 h. After the furnace was cooled to room temperature naturally, white wool-like matter was found to deposit on the Si wafer surface. Finally, the product was collected for further characterizations by FE-SEM (Hitachi S-4800), LEO 1550 SEM attached with an Oxford Inca Drycool EDS detector, and TEM (JEOL 4000EX).

Received: November 27, 2006
Revised: January 8, 2007
Published online: July 24, 2007

[1] *Nanowires and Nanobelts: Materials, Properties and Devices, Vol. I:, Metal and Semiconductor, Nanowires*, (Ed: Z. L. Wang), Kluwer Academic Publishers, New York **2003**.
[2] Z. L. Wang, X. Y. Kong, Y. Ding, P. X. Gao, W. Hughes, R. S. Yang, Y. Zhang, *Adv. Funct. Mater.* **2004**, *14*, 943.
[3] P. X. Gao, Z. L. Wang, *J. Appl. Phys.* **2005**, *97*, 044 304.
[4] X. Y. Kong, Y. Ding, R. Yang, Z. L. Wang, *Science* **2004**, *303*, 1348.
[5] X. Y. Kong, Z. L. Wang, *Nano Lett.* **2003**, *3*, 1625.
[6] P. X. Gao, Y. Ding, W. J. Mai, W. L. Hughes, C. S. Lao, Z. L. Wang, *Science* **2005**, *309*, 1700
[7] W. Hughes, Z. L. Wang, *J. Am. Chem. Soc.* **2004**, *126*, 6703.
[8] S. Hashimoto, A. Yamaguchi, *J. Am. Ceram. Soc.* **1996**, *79*, 1121.
[9] Z. L. Wang, X. Y. Kong, J. M. Zuo, *Phys. Rev. Lett.* **2003**, *91*, 185 502.
[10] Z. L. Wang, *Mater. Today* **2004**, *7(6)*, 26.
[11] D. Moore, Z. L. Wang, *J. Mater. Chem.* **2006**, *16*, 3898.
[12] D. Moore, Y. Ding, Z. L. Wang, *Angew. Chem. Int. Ed.* **2006**, *45*, 5150.
[13] C. Ma, D. Moore, J. Li, Z. L. Wang, *Adv. Mater,* **2003**, *15*, 228.
[14] O. G. Schmidt, N. Schmarje, C. Deneke, C. Müller, N. Y. J. Phillipp, *Adv. Mater.* **2001**, *13*, 756.
[15] O. G. Schmidt, C. Deneke, Y. M. Manz, C. Müller, *Phys. E* **2002**, *13*, 969.
[16] O. G. Schmidt, K. Eberl, *Nature* **2001**, *410*, 168.
[17] D. J. Bell, L. Dong, B. J. Nelson, M. Golling, L. Zhang, D. Grutzmacher, *Nano Lett.* **2006**, *6*, 725.
[18] L. Zhang, E. Ruh, D. Grutzmacher, L. X. Dong, D. J. Bell, B. J. Nelson, C. Schönenberger, *Nano Lett.* **2006**, *6*, 1311.

